

Trace of anomalous diffusion in a biased quenched trap model

Takuma Akimoto^{1,*} and Keiji Saito²

¹*Department of Physics, Tokyo University of Science, Noda, Chiba 278-8510, Japan*

²*Department of Physics, Keio University, Yokohama, 223-8522, Japan*

(Dated: August 1, 2021)

Diffusion on a quenched heterogeneous environment in the presence of bias is considered analytically. The first-passage-time statistics can be applied to obtain the drift and the diffusion coefficient in periodic quenched environments. We show several transition points at which sample-to-sample fluctuations of the drift or the diffusion coefficient remain large even when the system size becomes large, i.e., non-self-averaging. Moreover, we find that the disorder average of the diffusion coefficient diverges or becomes zero when the corresponding annealed model generates superdiffusion or subdiffusion, respectively. This result implies that anomalous diffusion in an annealed model is traced by anomaly of the diffusion coefficients in the corresponding quenched model.

I. INTRODUCTION

Anomalous transport characterized by a nonlinear growth of the mean squared displacement (MSD) or the mean displacement (MD) in the presence of bias is a ubiquitous phenomenon in nature. Since a discovery of anomalous transport in amorphous materials [1], considerable efforts have been made to unveil anomalous physical features in experiments such as biological systems [2–12]. One of physical mechanisms that produce anomalous transport is attributed to a heterogeneous environment, where local diffusivity is spatially heterogeneous or changes with time.

A typical model of anomalous diffusion on heterogeneous environments is a quenched trap model (QTM) [13]. In this model, the spatial heterogeneity is represented by a quenched random energy landscape. While this model is simple and has been investigated for decades, there are few exact results on the QTM [14]. This is because one has to take into account how a random walker visits a site. In particular, one needs to calculate the number of visits to a site by a random walker to obtain an exact result. The MSD of the QTM shows anomalous diffusion when the temperature is below the glass temperature, where the mean waiting time diverges [13]. By a scaling argument, it is known that the power-law exponent of the MSD depends on the spatial dimension [13]. Furthermore, fluctuations of the diffusion coefficients obtained by single trajectories depend intrinsically on the dimension [15, 16].

Continuous-time random walk (CTRW) is an annealed model of the QTM, which is widely used to investigate anomalous diffusion because its analytical treatment is possible due to the spatial homogeneity [17]. In the CTRW, the waiting-time distribution does not depend on the site but is identical for all the sites. This is a significant difference between the QTM and the CTRW, which gives a rich physical feature such as sample-to-sample fluctuations [15, 16, 18, 19]. However, the CTRW

becomes a good approximation of the QTM when the spatial dimension is greater than two or in the presence of bias [20]. In these situations, a random walker can visit a new site at constant non-zero probability, which reduces a risk of returning to the sites that a random walker visited before. Remarkable features of the CTRW are observed in the time-averaged-base MSD (TAMSD). When the mean waiting time diverges, the TAMSD is not coincided with the ensemble-averaged-base MSD, i.e., ergodicity breaking [21–24]. In our previous studies [19], we showed that the QTM with finite system size is ergodic; i.e., the TAMSD is equivalent to the corresponding MSD, and that the TAMSD becomes non-self-averaging when the temperature is below the glass temperature.

Effects of bias in the CTRW have been investigated in the regime where the mean waiting time is finite but the second moment diverges. In this regime, the drift is normal but the variance of the displacement (VD) shows superdiffusion, whereas the MSD in the absence of bias is normal [25, 26]. This phenomenon is called field-induced superdiffusion. Field-induced superdiffusion is ubiquitous phenomenon observed in crowded systems such as supercooled liquids [27–31]. However, field-induced superdiffusion in heterogeneous quenched environments has not been studied so far.

In this paper, we discuss how a bias affects transport properties in the QTM with a finite system size, where we assume a periodic boundary condition. In a periodic system, the first-passage-time (FPT) statistics plays an important role in obtaining the transport properties such as drift and diffusivity [32]. Applying the FPT statistics in a biased QTM [33], we show non-self-averaging properties of the MD and the VD. Comparing with the CTRW results, we provide an interesting connection between the annealed and quenched models.

II. MODEL

Here, we consider a random walk on a one-dimensional random energy landscape, i.e., QTM [13], where the energy landscape is quenched, and assume that the land-

* takuma@rs.tus.ac.jp

scape is arranged periodically. The probabilities of stepping to the right and the left site are denoted by p and $q = 1 - p$, respectively. We assume that the lattice constant is unity and that the tops of the potentials are flat; i.e., the tops are the same height for all sites. In other words, probabilities p and q do not depend on the site. In particular, we consider the case of $p \neq \frac{1}{2}$, i.e., a biased QTM, and $p > 1/2$ for simplicity.

Quenched disorder implies that when realizing the random energy landscape it does not change with time. The number of lattice sites with different energies is L ; i.e., the energy landscape of the system is periodically arranged with period L . At each lattice point, the depth $E > 0$ of an energy trap is randomly assigned and quenched. The depths are independent identically distributed random (IID) variables with an exponential distribution, $\rho(E) = T_g^{-1} \exp(-E/T_g)$, where T_g is called a glass temperature. A particle can escape from a trap and jump to one of the nearest neighbors. Escape times from a trap are IID random variables with an exponential distribution and follows the Arrhenius law; i.e., the mean escape time of the k th site is given by $\tau_k = \tau_c \exp(E_k/T)$, where E_k is the depth of the energy at site k , T the temperature, and τ_c a typical time. The probability that escape time τ is smaller than x is given by $\Pr(\tau \leq x) \cong \Pr(E \leq T \ln(x/\tau_c))$. Because the probability density function (PDF) of random variable E follows $\rho(E)$, the PDF of τ for infinite systems, denoted by $\psi_\alpha(\tau)$, becomes

$$\int_\tau^\infty d\tau' \psi_\alpha(\tau') \cong \left(\frac{\tau}{\tau_c}\right)^{-\alpha} \quad (\tau \geq \tau_c) \quad (1)$$

with $\alpha \equiv T/T_g$ [19, 34].

The master equation of the biased QTM can be represented by the quenched disorder realization. Let $P_k(t)$ be the probability of finding a particle at site k at time t . The master equation for the i th disorder realization, where the mean escape time at site k is denoted by $\tau_k^{(i)}$, is given by

$$\frac{dP_k(t)}{dt} = p \frac{P_{k-1}(t)}{\tau_{k-1}^{(i)}} + q \frac{P_{k+1}(t)}{\tau_{k+1}^{(i)}} - \frac{P_k(t)}{\tau_k^{(i)}}. \quad (2)$$

We consider the periodic boundary condition, i.e., $P_0(t) = P_L(t)$, $P_{L+1}(t) = P_1(t)$, $\tau_0^{(i)} = \tau_L^{(i)}$, and $\tau_{L+1}^{(i)} = \tau_1^{(i)}$. It follows that the steady state can be obtained as

$$P_k^{\text{st}} = \frac{\tau_k^{(i)}}{L\mu_i}, \quad (3)$$

where P_k^{st} is the probability of finding a particle at site k in the steady state and μ_i is the sample mean for the i th disorder realization:

$$\mu_i = \frac{1}{L} \sum_{k=0}^{L-1} \tau_k^{(i)}. \quad (4)$$

The steady state is exactly the same as the equilibrium state under no bias [19]. This is because the bias we consider here does not change the shape of the random energy landscape.

III. FIRST-PASSAGE-TIME STATISTICS AND DIFFUSIVE PROPERTIES

In our previous study [33], we derive the first-passage-time (FPT) statistics for the biased QTM. Here, we review the FPT statistics in the biased QTM and show that they play an important role in obtaining the diffusive properties such as drift and diffusivity in the system. The FPT in the biased QTM is defined as the time when a particle starting from the origin reaches site L , i.e., the right boundary. We note that the target is located at site L only (site $-L$ is not a target) whereas we consider a periodic landscape. In the large- L limit, the mean FPT (MFPT) and the variance of the FPT (VFPT) for the i th disorder realization are represented by

$$\langle T \rangle \sim \frac{L\mu_i}{p-q}, \quad (5)$$

$$\langle \delta T^2 \rangle \sim \frac{L\{\sigma_i^2(p-q) + \mu_i^2\}}{(p-q)^3}, \quad (6)$$

where $\delta T \equiv T - \langle T \rangle$ and σ_i^2 is the sample variance, i.e.,

$$\sigma_i^2 = \frac{1}{L} \sum_{n=0}^{L-1} (\tau_n^{(i)})^2 - \mu_i^2. \quad (7)$$

These formulae are exact for any quenched disorder realizations in the large- L limit and depend crucially on the disorder realization. Therefore, sample-to-sample fluctuations for the MFPT and the VFPT become significant when α is smaller than two [33].

Here, we connect the FPT statistics with the MD and the VD. Let n_t be the number of events that a particle crosses the right boundary, i.e., stepping from $L-1$ to L site, which is equivalent to make a counterclockwise revolution on a ring. In the large- L limit, the probability that a particle starting from the origin crosses the left boundary, i.e., stepping from $-L+1$ to $-L$ site, becomes zero. Therefore, a particle always resides in an interval $[(n_t-1)L, n_tL)$ in the large- L limit. It follows that the displacement, $\delta x_t \equiv x(t) - x(0)$, can be represented by

$$\delta x_t = Ln_t + C_L, \quad (8)$$

where $x(t)$ is a position of a particle at time t and C_L is a residual term that is considered to be a random variable whose support is $-L < C_L < L$, and thus $\langle |C_L| \rangle = O(L)$. Because time when a particle crosses the right boundary is an IID random variable, the process of n_t is described by a renewal process [35]. By the renewal theory [35], the mean of n_t is given by

$$\langle n_t \rangle \sim \frac{t}{\mu} \quad (t \rightarrow \infty), \quad (9)$$

where μ is the mean inter-event time, which is equivalent to MFPT $\langle T \rangle$. Therefore, the MD is represented by

$$\langle \delta x_t \rangle \sim \frac{L}{\langle T \rangle} t. \quad (10)$$

This formula is applicable for any diffusion processes when the landscape is periodic [32]. Applying the MFPT of the biased QTM, i.e., Eq. (5), we have

$$\langle \delta x_t \rangle \sim L \langle n_t \rangle \sim \frac{\varepsilon}{\mu_i} t \quad (t \rightarrow \infty), \quad (11)$$

where $\varepsilon = p - q$.

Using Eq. (8), we have

$$\delta x_t^2 = L^2 n_t^2 + 2LC_L n_t + C_L^2. \quad (12)$$

It follows that the variance of δx_t is given by

$$\langle \delta x_t^2 \rangle - \langle \delta x_t \rangle^2 \sim L^2 (\langle n_t^2 \rangle - \langle n_t \rangle^2) \quad (t \rightarrow \infty), \quad (13)$$

where we used a fact that C_L and n_t are independent, i.e., $\langle C_L n_t \rangle = \langle C_L \rangle \langle n_t \rangle$. By the renewal theory [35], the variance of n_t is derived for $t \gg 1$ as

$$\langle n_t^2 \rangle - \langle n_t \rangle^2 \sim \frac{\langle T^2 \rangle - \langle T \rangle^2}{\langle T \rangle^3} t, \quad (14)$$

where $\langle T^2 \rangle$ is the second moment of the FPT. Therefore, the variance of δx_t can be represented by

$$\langle \delta x_t^2 \rangle - \langle \delta x_t \rangle^2 \sim \left(\frac{\varepsilon \sigma_i^2}{\mu_i^3} + \frac{1}{\mu_i} \right) t \quad (15)$$

for $t \rightarrow \infty$. Figure 2 shows a good agreement in between numerical simulations and the theory.

IV. SELF-AVERAGING PROPERTIES FOR DRIFT AND DIFFUSIVITY

A. Drift

The asymptotic behavior of the MD is given by Eq. (11). The result becomes exact for any $t > 0$ when the initial condition is the steady state of the system, i.e., Eq. (3), because the MD can be described as

$$\langle \delta x_t \rangle_{\text{st}} = \varepsilon \langle N_t \rangle_{\text{st}} \quad (16)$$

for any $t > 0$, where N_t is the mean number of steps of a particle until time t and $\langle \cdot \rangle_{\text{st}}$ is the average when the initial condition is the steady state. When the initial condition is the steady state, $\langle N_t \rangle_{\text{st}}$ increases linearly with time:

$$\langle N_t \rangle_{\text{st}} = \frac{t}{\mu_i} \quad (17)$$

for any $t > 0$. Hence, the drift defined as $\lambda \equiv \langle \delta x_t \rangle_{\text{st}} / t$ is given by

$$\lambda_i(L) = \frac{\varepsilon}{\mu_i} \quad (18)$$

for some disorder realization.

Now, we consider sample-to-sample fluctuations of the drift. When the mean trapping time, $\langle \tau \rangle \equiv \int_0^\infty \tau \psi_\alpha(\tau) d\tau$, is finite ($\alpha > 1$), we have $\mu_i \rightarrow \langle \tau \rangle$ ($L \rightarrow \infty$) by the law of large numbers. Therefore, in the large- L limit, the drift does not depend on the disorder realization (see Fig. 1). Hence, the drift is self-averaging (SA) for $\alpha > 1$ [13]. To quantify the SA property of λ_i , we consider the SA parameter defined as [19]

$$\text{SA}(L; \lambda) \equiv \frac{\langle \lambda_i(L)^2 \rangle_{\text{dis}} - \langle \lambda_i(L) \rangle_{\text{dis}}^2}{\langle \lambda_i(L) \rangle_{\text{dis}}^2}, \quad (19)$$

where $\langle \cdot \rangle_{\text{dis}}$ means the disorder average, i.e., the average obtained under different disorder realizations. The SA parameter becomes zero in the large- L limit when the drift is SA. Using Eq. (18), we have

$$\text{SA}(L; \lambda) = \frac{\langle 1/\mu_i^2 \rangle_{\text{dis}} - \langle 1/\mu_i \rangle_{\text{dis}}^2}{\langle 1/\mu_i \rangle_{\text{dis}}^2}, \quad (20)$$

which is the same as the SA parameter for the diffusion coefficient in the absence of bias [19]. For $\alpha > 2$, the SA parameter decays as L^{-1} by the central limit theorem. For $1 < \alpha < 2$, it goes to zero as $L \rightarrow \infty$ by the law large numbers. However, as shown in Appendix. A, it decays non-trivially as $L^{-\alpha+1}$ in the large- L limit. Therefore, sample-to-sample fluctuations remain large even for a relatively large L when α closes to one.

When the mean trapping time diverges ($\alpha \leq 1$), the law of large numbers does not hold. However, the generalized central limit theorem is still valid, which states that the PDF of the normalized sum of $\tau_n^{(i)}$ follows the one-sided Lévy distribution [36]:

$$\frac{\sum_{n=1}^L \tau_n^{(i)}}{L^{1/\alpha}} \Rightarrow X_\alpha \quad (L \rightarrow \infty), \quad (21)$$

where X_α is a random variable following the one-sided Lévy distribution of index α . Therefore, there are large sample-to-sample fluctuations in sample mean μ_i . The PDF of X_α , denoted by $l_\alpha(x)$ with $x > 0$, can be expressed as an infinite series [36]

$$l_\alpha(x) = -\frac{1}{\pi x} \sum_{k=1}^{\infty} \frac{\Gamma(k\alpha + 1)}{k!} (-cx^{-\alpha})^k \sin(k\pi\alpha), \quad (22)$$

where c is a scale parameter, given by $c = \Gamma(1 - \alpha) \tau_c^\alpha$ for $\psi_\alpha(\tau)$. Here, we define the inverse Lévy distribution as the PDF of X_α^{-1} :

$$g_\alpha(y) = -\frac{1}{\pi y} \sum_{k=1}^{\infty} \frac{\Gamma(k\alpha + 1)}{k!} (-cy^\alpha)^k \sin(k\pi\alpha), \quad (23)$$

where the first and the second moments of X_α^{-1} are given by [19]

$$\langle X_\alpha^{-1} \rangle = \frac{\Gamma(\frac{1}{\alpha})}{\alpha c^{\frac{1}{\alpha}}}, \quad \langle X_\alpha^{-2} \rangle = \frac{\Gamma(\frac{2}{\alpha})}{\alpha c^{\frac{2}{\alpha}}}. \quad (24)$$

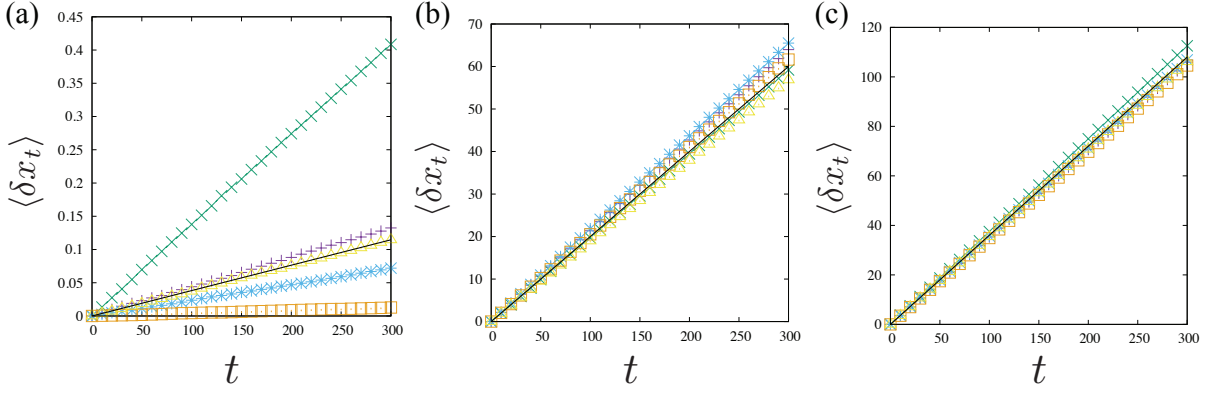


FIG. 1. Mean displacement (MD) for different α (a) $\alpha = 0.5$, (b) $\alpha = 1.5$, and (c) $\alpha = 2.5$ ($p = 0.8$ and $\tau_c = 1$). Symbols are the results of MDs for five different disorder realizations ($L = 10^3$). We note that the average is taken only for the thermal average. Thus, sample-to-sample fluctuations are significant for (a). Solid lines are the disorder averages of the MD, i.e., $\langle \lambda \rangle_{\text{dis}} t$, where $\langle \lambda \rangle_{\text{dis}}$ can be calculated by Eq. (26) for $\alpha \leq 1$ and $\langle \lambda \rangle_{\text{dis}} = \varepsilon / \langle \mu \rangle_{\text{dis}}$ for $\alpha > 1$, which can be calculated by Eq. (1).

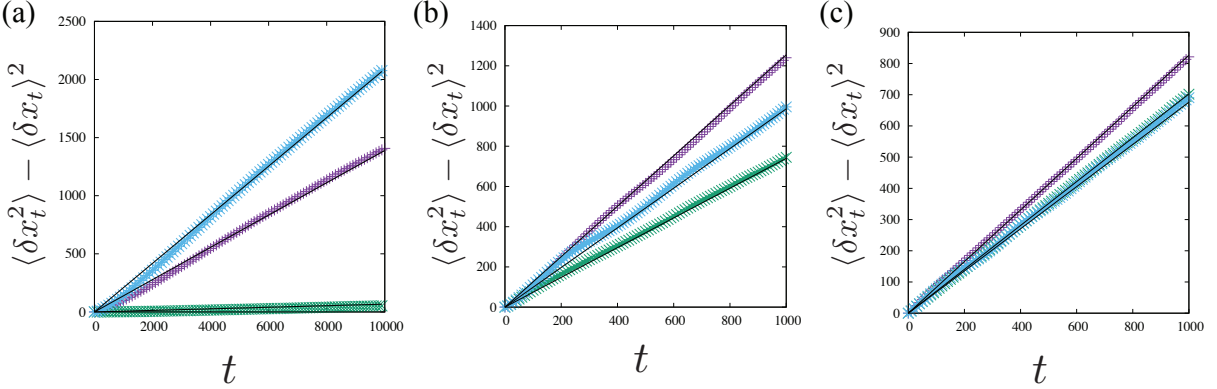


FIG. 2. Variance of the displacement (VD) for different α (a) $\alpha = 0.5$, (b) $\alpha = 1.5$, and (c) $\alpha = 2.5$ ($p = 0.8$ and $\tau_c = 1$). Symbols are the results of VDs for three different disorder realizations ($L = 10^2$). Solid lines are the asymptotic results, i.e., Eq. (15).

Drift can be represented by

$$\lambda_i(L) = \varepsilon \frac{L}{L^{1/\alpha} \tau_1 + \dots + \tau_L} \sim \varepsilon L^{1-1/\alpha} X_\alpha^{-1} \quad (25)$$

for $L \rightarrow \infty$. Thus, the PDF of λ_i is described by the inverse Lévy distribution. Therefore, λ_i depends crucially on the sample of the disorder realization. Using the first moment of the inverse Lévy distribution [19], we obtain the exact asymptotic behavior of the disorder average of the drift:

$$\langle \lambda(L) \rangle_{\text{dis}} \sim \frac{\varepsilon L^{1-1/\alpha} \Gamma(\alpha^{-1})}{\alpha \tau_c \Gamma(1-\alpha)^{1/\alpha}}. \quad (26)$$

Using the first and the second moment of $1/\mu_i$, we have the SA parameter for drift

$$\lim_{L \rightarrow \infty} \text{SA}(L; \lambda) = \begin{cases} 0 & (\alpha > 1) \\ \frac{\alpha \Gamma(\frac{2}{\alpha})}{\Gamma(\frac{1}{\alpha})^2} - 1 & (\alpha \leq 1). \end{cases} \quad (27)$$

For $\alpha < 1$, the SA parameter is a non-zero constant, and thus λ_i becomes non-SA; i.e., there are large sample-to-sample fluctuations in the drift [see Fig. 1(a)]. Therefore, the transition temperature from SA to non-SA behavior in the drift is given by $T_c = T_g$.

B. Diffusivity

Here, we consider the VD to characterize the diffusivity of the system, which is defined as

$$\text{Var}(\delta x_t)_{\text{st}} \equiv \langle \delta x_t^2 \rangle_{\text{st}} - \langle \delta x_t \rangle_{\text{st}}^2. \quad (28)$$

By Eq. (15), the asymptotic behavior of the VD increases linearly with time:

$$\text{Var}(\delta x_t)_{\text{st}} \sim \left(\frac{\varepsilon \sigma_i^2}{\mu_i^3} + \frac{1}{\mu_i} \right) t \quad (29)$$

for $t \gg 1$ and $L \gg 1$. Therefore, the diffusion coefficient of the system, i.e., $D_i(L) \equiv \lim_{t \rightarrow \infty} \text{Var}(\delta x_t)_{\text{st}} / (2t)$, is given by

$$D_i(L) \sim \frac{1}{2} \left(\frac{\varepsilon \sigma_i^2}{\mu_i^3} + \frac{1}{\mu_i} \right) \quad (30)$$

for $L \rightarrow \infty$. The disorder average of $D_i(L)$ is given by

$$\langle D(L) \rangle_{\text{dis}} \sim \frac{1}{2} \left(\varepsilon \left\langle \frac{\sigma_i^2}{\mu_i^3} \right\rangle_{\text{dis}} + \left\langle \frac{1}{\mu_i} \right\rangle_{\text{dis}} \right) \quad (31)$$

for $L \rightarrow \infty$. For $\alpha > 2$, the second moment of trapping times exists; i.e., $\langle \tau^2 \rangle \equiv \int_0^\infty \tau^2 \psi(\tau) d\tau < \infty$. It follows that the disorder average of $D_i(L)$ is finite and given by

$$\langle D(L) \rangle_{\text{dis}} \sim \frac{1}{2} \left(\varepsilon \frac{\langle \tau^2 \rangle - \langle \tau \rangle^2}{\langle \tau \rangle^3} + \frac{1}{\langle \tau \rangle} \right) \quad (32)$$

for $L \rightarrow \infty$ and $\alpha > 2$.

For $\alpha < 2$, the disorder average of $\{\tau_n^{(i)}\}^2$ diverges. To compute the disorder average of σ_i^2 / μ_i^3 , we consider the scaling of the sum of $\{\tau_n^{(i)}\}^2$. The PDF of $\{\tau_n^{(i)}\}^2$ is given by

$$\psi_{2,\alpha}(x) = \frac{1}{2\sqrt{x}} \psi_\alpha(\sqrt{x}), \quad (33)$$

because $\text{Pr}(\tau^2 \leq x) = \text{Pr}(\tau \leq \sqrt{x}) = \int_0^{\sqrt{x}} \psi_\alpha(x') dx'$. For $x \rightarrow \infty$, the PDF becomes

$$\psi_{2,\alpha}(x) \propto x^{-1-\alpha/2} \propto \psi_{\alpha/2}(x). \quad (34)$$

By the generalized central limit theorem [36], normalized sum $X_{\frac{\alpha}{2}}(L)$, defined by

$$X_{\frac{\alpha}{2}}(L) \equiv \frac{1}{L^{2/\alpha}} \sum_{n=1}^L \{\tau_n^{(i)}\}^2, \quad (35)$$

converges in distribution to a random variable with the one-sided Lévy distribution of index $\alpha/2$. For $1 < \alpha < 2$, $\langle \tau \rangle$ is finite but $\langle \tau^2 \rangle$ diverges. Therefore, $D_i(L)$ is proportional to σ_i^2 / μ_i^3 , which depends on L . As shown in Appendix B, the disorder average of $D_i(L)$ increases with L :

$$\langle D(L) \rangle_{\text{dis}} \propto L^{2-\alpha} \quad (36)$$

for $L \rightarrow \infty$, which means that the diffusion coefficient diverges in the large- L limit [see Fig. 3(b)]. This divergence of the diffusion coefficient is a manifestation of field-induced superdiffusion in the corresponding annealed system, i.e., the biased CTRW [25]. This is because the variance of the displacement exhibits superdiffusion, i.e., $\text{Var}(\delta x_t)_{\text{st}} \propto t^{3-\alpha}$, which means that a standard diffusion coefficient diverges.

For $\alpha < 1$, both the first and the second moments of the trapping times diverge. The scalings of the sums of $\tau_n^{(i)}$ and $\{\tau_n^{(i)}\}^2$ follows

$$\sum_{n=1}^L \tau_n = O(L^{1/\alpha}) \quad \text{and} \quad \sum_{n=1}^L \{\tau_n^{(i)}\}^2 = O(L^{2/\alpha}) \quad (37)$$

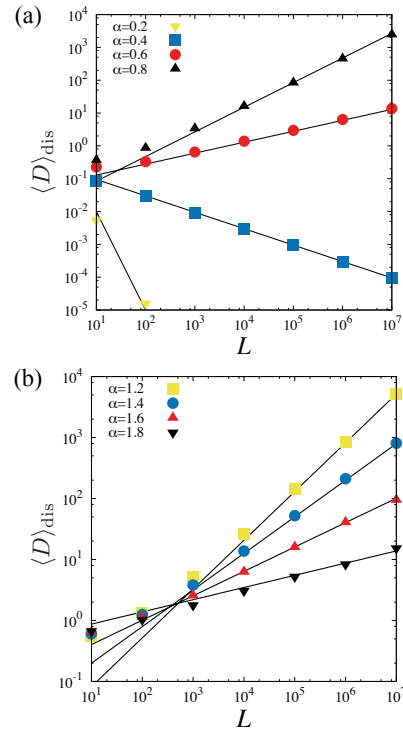


FIG. 3. Disorder average of the diffusion coefficient as a function of L for different α ($p = 0.8$ and $\tau_c = 1$). Symbols are the results of numerical simulations. Solid lines are the asymptotic results, i.e., Eqs. (36) and (39).

for $L \rightarrow \infty$. Since $D_i(L)$ is proportional to σ_i^2 / μ_i^3 , we have

$$D_i(L) \propto \frac{\sigma_i^2}{\mu_i^3} \propto L^2 \frac{\sum_{n=1}^L \tau_n^2}{(\sum_{n=1}^L \tau_n)^3} \propto L^{2-1/\alpha}. \quad (38)$$

It follows that the scaling of the disorder average of $D_i(L)$ becomes

$$\langle D(L) \rangle_{\text{dis}} \propto L^{2-1/\alpha} \quad (39)$$

Hence, the diffusion coefficient diverges for $\alpha > 1/2$, whereas it becomes zero for $\alpha < 1/2$ [see Fig. 3(a)]. This is physically reasonable because the variance of the displacement in the CTRW with drift becomes superdiffusive and subdiffusive for $\alpha > 1/2$ and $\alpha < 1/2$, respectively.

Let us consider the SA property for the diffusion coefficient. The SA parameter is defined as

$$\text{SA}(L; D) \equiv \frac{\langle D(L)^2 \rangle_{\text{dis}} - \langle D(L) \rangle_{\text{dis}}^2}{\langle D(L) \rangle_{\text{dis}}^2}. \quad (40)$$

The SA parameter goes to zero in the large- L limit when the diffusion coefficient is SA.

For $\alpha > 2$, the second moment of trapping times exists; i.e., $\langle \tau^2 \rangle \equiv \int_0^\infty \tau^2 \psi(\tau) d\tau < \infty$. Therefore, sample variance σ_i^2 converges to $\langle \tau^2 \rangle - \langle \tau \rangle^2$ as $L \rightarrow \infty$. Hence,

the sample mean and the sample mean of the squared trapping times are converges to constants, which means $\langle D(L)^2 \rangle_{\text{dis}} - \langle D(L) \rangle_{\text{dis}}^2 \rightarrow 0$ for $L \rightarrow \infty$. Therefore, the diffusion coefficient is SA for $\alpha > 2$.

For $1 < \alpha < 2$, the second moment of $D_i(L)$ is also calculated in Appendix. B. As shown in Fig. 4(b), the SA parameter increases with L . In particular, it diverges as

$$\text{SA}(L; D) \propto \frac{\langle D(L)^2 \rangle_{\text{dis}}}{\langle D(L) \rangle_{\text{dis}}^2} \propto L^{\alpha-1} \quad (41)$$

for $L \rightarrow \infty$. It follows that the diffusion coefficient is non-SA for $1 < \alpha < 2$.

For $\alpha < 1$, both the first and the second moment of the trapping times diverge. By Eq. (38) and $\sum_{n=1}^L \tau_n^2 < \left(\sum_{n=1}^L \tau_n\right)^3$, $D_i(L)$ can be represented as

$$D_i(L) \sim \frac{\varepsilon L^{2-1/\alpha}}{2} C_i(L), \quad (42)$$

where $C_i(L) = L^{1/\alpha} \sum_{n=1}^L \tau_n^2 / \left(\sum_{n=1}^L \tau_n\right)^3$ is a random variable depending on the disorder realization. Therefore, the SA parameter becomes

$$\text{SA}(L; D) = \frac{\langle D(L)^2 \rangle_{\text{dis}}}{\langle D(L) \rangle_{\text{dis}}^2} - 1 = \frac{\langle C(L)^2 \rangle_{\text{dis}}}{\langle C(L) \rangle_{\text{dis}}^2} - 1, \quad (43)$$

which is a finite value because $1 / \left(\sum_{n=1}^L \tau_n\right)^3 < C_i(L) < 1$, i.e., $0 < \langle C_i(L) \rangle_{\text{dis}} < 1$ and $0 < \langle C_i(L)^2 \rangle_{\text{dis}} < 1$. Thus, $\text{SA}(L; D) \rightarrow S(\alpha) > 0$ for $L \rightarrow \infty$; i.e., the diffusion coefficient is non-SA for $\alpha < 1$ [see Fig. 4(a)].

V. CONCLUSION

The MD and the VD are always normal in a biased QTM with a finite system size with the aid of a stationary steady state, which is different from the biased CTRW. Using the FPT statistics, we have provided exact results for the drift and the diffusion coefficient in the biased QTM. We have found that anomaly of the disorder average of the diffusion coefficient is a manifestation of anomalous diffusion in the corresponding annealed model (CTRW). In particular, divergence and zero of the disorder average of the diffusion coefficient, i.e., $\langle D \rangle_{\text{dis}}$, in the biased QTM implies superdiffusion and subdiffusion in the biased CTRW, respectively (see Fig. 5). Moreover, we have introduced the SA parameter to quantify the SA property. Transition points between SA and non-SA are $\alpha = 1$ and $\alpha = 2$ for the MD and the VD, respectively.

ACKNOWLEDGEMENT

T.A. was supported by JSPS Grant-in-Aid for Scientific Research (No. C JP18K03468) and K.S. was supported by JSPS Grants-inAid for Scientific Research (JP17K05587).

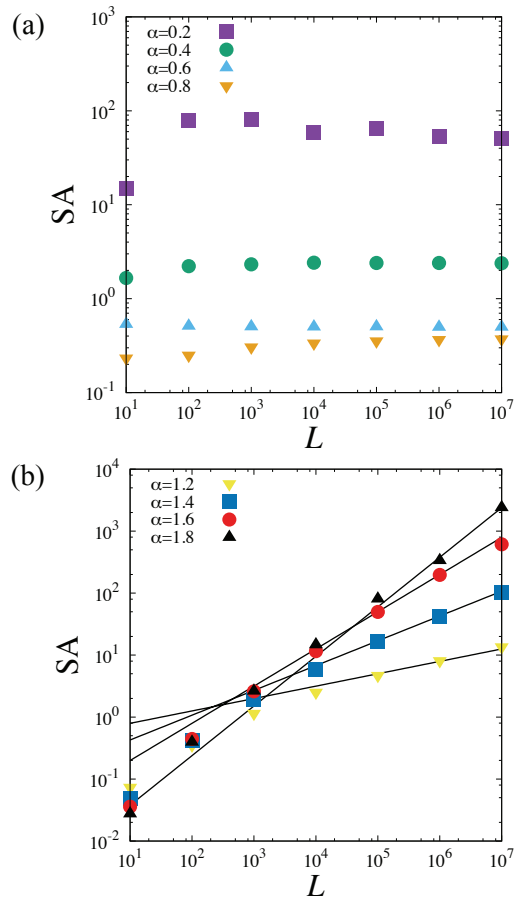


FIG. 4. Self-averaging parameter of the diffusion coefficient as a function of L for different α ($p = 0.8$ and $\tau_c = 1$). Symbols are the results of numerical simulations. Solid lines are the asymptotic results, i.e., Eq. (41).

Appendix A: Scaling of the SA parameter for drift

Here, we show a power-law decay of the SA parameter for drift. For $1 < \alpha < 2$, it decays as $L^{1-\alpha}$, where L is the system size. Drift for a sample realization is given by

$$\lambda(L) = \frac{\varepsilon L}{\tau_1 + \dots + \tau_L} = \frac{\varepsilon L}{L^{1/\alpha} \tilde{X}_\alpha(L) + \langle \tau \rangle L}, \quad (A1)$$

where

$$\tilde{X}_\alpha(L) = \frac{\tau_1 + \dots + \tau_L - \langle \tau \rangle L}{L^{1/\alpha}}. \quad (A2)$$

In the large- L limit, the PDF of $\tilde{X}_\alpha(L)$ converges to the Lévy distribution of index α . For $L^{1/\alpha-1} \tilde{X}_\alpha(L) \ll \langle \tau \rangle \varepsilon$, $\lambda(L)$ becomes

$$\lambda(L) \cong \frac{\varepsilon}{\langle \tau \rangle} - \frac{\varepsilon L^{1/\alpha-1} \tilde{X}_\alpha(L)}{\langle \tau \rangle^2}. \quad (A3)$$

On the other hand, it becomes

$$\lambda(L) \cong \frac{\varepsilon L^{1-1/\alpha}}{\tilde{X}_\alpha(L)} \quad (A4)$$

CTRW	subdiffusion (nonergodic)	superdiffusion (nonergodic)	superdiffusion (ergodic)	normal (ergodic)
	normal (non-SA) $\langle D \rangle_{\text{dis}} = 0$	normal (non-SA) $\langle D \rangle_{\text{dis}} = \infty$	normal (non-SA) $\langle D \rangle_{\text{dis}} = \infty$	normal (SA) $\langle D \rangle_{\text{dis}} < \infty$
QTM				
	0	$\frac{1}{2}$	1	2
	α			

FIG. 5. Phase diagram based on diffusivity in the CTRW and QTM. Divergence of the disorder average of the diffusion coefficient in the large- L limit implies superdiffusion in the CTRW. On the other hand, zero of the disorder average of the diffusion coefficient implies subdiffusion in the CTRW. Note that ergodicity in the CTRW does not imply SA in the corresponding quenched model.

for $L^{1/\alpha-1}\tilde{X}_\alpha(L) \gg \langle \tau \rangle \varepsilon$. The ensemble average of $\tilde{X}_\alpha(L)^2$ restricted in $\tilde{X}_\alpha(L) < L^{1-1/\alpha}\langle \tau \rangle \varepsilon$, denoted by $\langle \tilde{X}_\alpha(L)^2 \rangle_{<L^{1-1/\alpha}}$, is given by

$$\langle \tilde{X}_\alpha(L)^2 \rangle_{<L^{1-1/\alpha}} \cong \int_0^{L^{1-1/\alpha}\langle \tau \rangle \varepsilon} x^2 \psi_\alpha(x) dx \quad (\text{A5})$$

$$\propto L^{3-\frac{2}{\alpha}-\alpha}. \quad (\text{A6})$$

Moreover, the ensemble average of $1/\tilde{X}_\alpha(L)^2$ restricted in $\tilde{X}_\alpha(L) > L^{1-1/\alpha}\langle \tau \rangle \varepsilon$, denoted by $\langle 1/\tilde{X}_\alpha(L)^2 \rangle_{>L^{1-1/\alpha}}$, is given by

$$\langle \tilde{X}_\alpha(L)^{-2} \rangle_{>L^{1-1/\alpha}} \cong \int_{L^{1-1/\alpha}\langle \tau \rangle \varepsilon}^{\infty} x^{-2} \psi_\alpha(x) dx \quad (\text{A7})$$

$$\propto L^{-(2+\alpha)(1-\frac{1}{\alpha})}. \quad (\text{A8})$$

The variance of $\lambda(L)$ becomes

$$\langle \lambda(L)^2 \rangle_{\text{dis}} - \langle \lambda(L) \rangle_{\text{dis}}^2 \propto L^{\frac{2}{\alpha}-2} \langle \tilde{X}_\alpha(L)^2 \rangle_{<L^{1-1/\alpha}} + L^{2-\frac{2}{\alpha}} \langle \tilde{X}_\alpha(L)^{-2} \rangle_{>L^{1-1/\alpha}}. \quad (\text{A9})$$

It follows that the scaling of the SA parameter for drift becomes

$$\text{SA}(L; \lambda) \propto L^{1-\alpha} \quad (\text{A10})$$

for $L \rightarrow \infty$ and $1 < \alpha < 2$.

Appendix B: Scaling for the SA parameter for diffusivity

For $1 < \alpha < 2$, the diffusion coefficient is proportional to σ_i^2/μ_i^3 , which can be written as

$$\frac{\sigma_i^2}{\mu_i^3} = \frac{(\tau_1^2 + \dots + \tau_L^2)L^2}{\langle \tau \rangle^3 L^3 \left(1 + \frac{L^{1/\alpha-1}}{\langle \tau \rangle} \tilde{X}_\alpha(L)\right)^3}. \quad (\text{B1})$$

For $\tilde{X}_\alpha(L) \ll L^{1-1/\alpha}\langle \tau \rangle$,

$$\frac{\sigma_i^2}{\mu_i^3} \propto \frac{\tau_1^2 + \dots + \tau_L^2}{L} = L^{\frac{\alpha}{2}-1} X_{\frac{\alpha}{2}}(L) \quad (\text{B2})$$

in the large- L limit. Moreover, variable $X_{\frac{\alpha}{2}}(L)$ satisfies

$$X_{\frac{\alpha}{2}}(L) < \frac{(\tau_1 + \dots + \tau_L)^2}{L^{2/\alpha}} \sim \langle \tau \rangle^2 L^{2-\frac{2}{\alpha}} \quad (\text{B3})$$

for $\tilde{X}_\alpha(L) \ll L^{1-1/\alpha}\langle \tau \rangle$. Scaling of the disorder average of D_i follows

$$\left\langle \frac{\sigma_i^2}{\mu_i^3} \right\rangle_{\text{dis}} \propto L^{\frac{2}{\alpha}-1} \langle X_{\frac{\alpha}{2}}(L) \rangle_{<L^{2-\frac{2}{\alpha}}} + L^{2-\frac{3}{\alpha}} \left\langle \frac{X_{\frac{\alpha}{2}}(L)}{\tilde{X}_\alpha(L)^3} \right\rangle_{>L^{2-\frac{2}{\alpha}}}, \quad (\text{B4})$$

where $\langle \cdot \rangle_{<L^{2-\frac{2}{\alpha}}}$ and $\langle \cdot \rangle_{>L^{2-\frac{2}{\alpha}}}$ represent the ensemble averages restricted in $X_{\frac{\alpha}{2}}(L) < L^{2-\frac{2}{\alpha}}$ and $X_{\frac{\alpha}{2}}(L) > L^{2-\frac{2}{\alpha}}$, respectively. Using Eq. (B3), we obtain $L^{\frac{2}{\alpha}-1} \langle X_{\frac{\alpha}{2}}(L) \rangle_{<L^{2-\frac{2}{\alpha}}} \propto L^{2-\alpha}$. The second term can be evaluated as

$$\left\langle \frac{X_{\frac{\alpha}{2}}(L)}{\tilde{X}_\alpha(L)^3} \right\rangle_{>L^{2-\frac{2}{\alpha}}} < \left\langle \frac{1}{\tilde{X}_\alpha(L)} \right\rangle_{>L^{1-\frac{1}{\alpha}}}. \quad (\text{B5})$$

Thus, the second term can be neglected because the order is smaller than the first one, i.e., $L^{2-\alpha}$. It follows that the scaling of the disorder average of D_i becomes

$$\langle D(L) \rangle_{\text{dis}} \propto \left\langle \frac{\sigma_i^2}{\mu_i^3} \right\rangle_{\text{dis}} \propto L^{2-\alpha}. \quad (\text{B6})$$

By Eq. (B2), one obtains the second moment of $D_i(L)$ in a similar way. It becomes

$$\langle D(L)^2 \rangle_{\text{dis}} \propto L^{2(\frac{2}{\alpha}-1)} \langle X_{\frac{\alpha}{2}}(L)^2 \rangle_{L^{2-\frac{2}{\alpha}}} \quad (\text{B7})$$

for $L \rightarrow \infty$. Therefore, the SA parameter for the diffusion coefficient is given by

$$\text{SA}(L; D) \propto \frac{\langle D(L)^2 \rangle_{\text{dis}}}{\langle D(L) \rangle_{\text{dis}}^2} \propto L^{\alpha-1} \quad (\text{B8})$$

for $L \rightarrow \infty$ and $1 < \alpha < 2$.

-
- [1] H. Scher and E. W. Montroll, *Phys. Rev. B* **12**, 2455 (1975).
- [2] A. Caspi, R. Granek, and M. Elbaum, *Phys. Rev. Lett.* **85**, 5655 (2000).
- [3] I. Y. Wong, M. L. Gardel, D. R. Reichman, E. R. Weeks, M. T. Valentine, A. R. Bausch, and D. A. Weitz, *Phys. Rev. Lett.* **92**, 178101 (2004).
- [4] I. Golding and E. C. Cox, *Phys. Rev. Lett.* **96**, 098102 (2006).
- [5] J. Szymanski and M. Weiss, *Phys. Rev. Lett.* **103**, 038102 (2009).
- [6] I. Bronstein, Y. Israel, E. Kepten, S. Mai, Y. Shav-Tal, E. Barkai, and Y. Garini, *Phys. Rev. Lett.* **103**, 018102 (2009).
- [7] N. Gal and D. Weihs, *Phys. Rev. E* **81**, 020903 (2010).
- [8] A. Weigel, B. Simon, M. Tamkun, and D. Krapf, *Proc. Natl. Acad. Sci. USA* **108**, 6438 (2011).
- [9] J.-H. Jeon, V. Tejedor, S. Burov, E. Barkai, C. Selhuber-Unkel, K. Berg-Sørensen, L. Oddershede, and R. Metzler, *Phys. Rev. Lett.* **106**, 048103 (2011).
- [10] S. A. Tabei, S. Burov, H. Y. Kim, A. Kuznetsov, T. Huynh, J. Jureller, L. H. Philipson, A. R. Dinner, and N. F. Scherer, *Proc. Natl. Acad. Sci. USA* **110**, 4911 (2013).
- [11] F. Höfling and T. Franosch, *Rep. Prog. Phys.* **76**, 046602 (2013).
- [12] C. Manzo, J. A. Torreno-Pina, P. Massignan, G. J. Lapeyre Jr, M. Lewenstein, and M. F. G. Parajo, *Phys. Rev. X* **5**, 011021 (2015).
- [13] J. Bouchaud and A. Georges, *Phys. Rep.* **195**, 127 (1990).
- [14] B. Derrida, *J. Stat. Phys.* **31**, 433 (1983).
- [15] T. Miyaguchi and T. Akimoto, *Phys. Rev. E* **83**, 031926 (2011).
- [16] T. Miyaguchi and T. Akimoto, *Phys. Rev. E* **91**, 010102(R) (2015).
- [17] R. Metzler and J. Klafter, *Phys. Rep.* **339**, 1 (2000).
- [18] L. Luo and L.-H. Tang, *Phys. Rev. E* **92**, 042137 (2015).
- [19] T. Akimoto, E. Barkai, and K. Saito, *Phys. Rev. Lett.* **117**, 180602 (2016); *Phys. Rev. E* **97**, 052143 (2018).
- [20] J. Machta, *Journal of Physics A: Mathematical and General* **18**, L531 (1985).
- [21] Y. He, S. Burov, R. Metzler, and E. Barkai, *Phys. Rev. Lett.* **101**, 058101 (2008).
- [22] T. Neusius, I. M. Sokolov, and J. C. Smith, *Phys. Rev. E* **80**, 011109 (2009).
- [23] T. Miyaguchi and T. Akimoto, *Phys. Rev. E* **87**, 032130 (2013).
- [24] R. Metzler, J.-H. Jeon, A. G. Cherstvy, and E. Barkai, *Phys. Chem. Chem. Phys.* **16**, 24128 (2014).
- [25] R. Burioni, G. Gradenigo, A. Sarracino, A. Vezzani, and A. Vulpiani, *J. Stat. Mech.*, P09022 (2013); *Commun. Theor. Phys.* **62**, 514 (2014).
- [26] T. Akimoto, A. G. Cherstvy, and R. Metzler, *Phys. Rev. E* **98**, 022105 (2018); R. Hou, A. G. Cherstvy, R. Metzler, and T. Akimoto, *Phys. Chem. Chem. Phys.* **20**, 20827 (2018).
- [27] C. F. E. Schroer and A. Heuer, *Phys. Rev. Lett.* **110**, 067801 (2013).
- [28] O. Bénichou, A. Bodrova, D. Chakraborty, P. Illien, A. Law, C. Mejía-Monasterio, G. Oshanin, and R. Voituriez, *Phys. Rev. Lett.* **111**, 260601 (2013).
- [29] O. Bénichou, P. Illien, C. Mejía-Monasterio, and G. Oshanin, *J. Stat. Mech.* **2013**, P05008.
- [30] G. Gradenigo, E. Bertin, and G. Biroli, *Phys. Rev. E* **93**, 060105 (2016).
- [31] S. Leitmann and T. Franosch, *Phys. Rev. Lett.* **118**, 018001 (2017).
- [32] P. Reimann, C. Van den Broeck, H. Linke, P. Hänggi, J. M. Rubi, and A. Pérez-Madrid, *Phys. Rev. Lett.* **87**, 010602 (2001); *Phys. Rev. E* **65**, 031104 (2002).
- [33] T. Akimoto and K. Saito, *Phys. Rev. E* **99**, 052127 (2019).
- [34] F. Bardou, J.-P. Bouchaud, A. Aspect, and C. Cohen-Tannoudji, *Levy statistics and laser cooling: how rare events bring atoms to rest* (Cambridge University Press, 2002).
- [35] D. R. Cox, *Renewal theory* (Methuen, London, 1962).
- [36] W. Feller, *An Introduction to Probability Theory and its Applications*, 2nd ed., Vol. 2 (Wiley, New York, 1971).